Available online at www.sciencedirect.com
ScienceDirect
Journal of Computational Physics 227 (2008) 7178–7191
JOURNAL OF COMPUTATIONAL PHYSICS
www.elsevier.com/locate/jcp

A full vectorial generalized discontinuous Galerkin beam propagation method (GDG–BPM) for nonsmooth electromagnetic fields in waveguides

Kai Fan, Wei Cai *, Xia Ji

Department of Mathematics and Statistics, University of North Carolina at Charlotte, Charlotte, NC 28223, United States

Received 12 November 2007; received in revised form 30 January 2008; accepted 21 March 2008
Available online 15 April 2008

Abstract

In this paper, we propose a new full vectorial generalized discontinuous Galerkin beam propagation method (GDG–BPM) to accurately handle the discontinuities in electromagnetic fields associated with wave propagations in inhomogeneous optical waveguides. The numerical method is a combination of the traditional beam propagation method (BPM) with a newly developed generalized discontinuous Galerkin (GDG) method [K. Fan, W. Cai, X. Ji, A generalized discontinuous Galerkin method (GDG) for Schrödinger equations with nonsmooth solutions, J. Comput. Phys. 227 (2008) 2387–2410]. The GDG method is based on a reformulation, using distributional variables to account for solution jumps across material interfaces, of Schrödinger equations resulting from paraxial approximations of vector Helmholtz equations. Four versions of the GDG–BPM are obtained for either the electric or magnetic field components. Modeling of wave propagations in various optical fibers using the full vectorial GDG–BPM is included. Numerical results validate the high order accuracy and the flexibility of the method for various types of interface jump conditions.

MSC: 65N38; 78M25

Keywords: Discontinuous Galerkin method; Beam propagation method; Inhomogeneous optical waveguide, Dirac δ source; Schrödinger equation

1. Introduction

In beam propagation methods (BPM) [1,2] using paraxial approximations for wave propagations in optical waveguides, time harmonic Maxwell's equations are approximated by Schrödinger equations where the propagation direction is treated as the time axis. Due to the mismatch of refractive indices in the cross section of the waveguides, the electromagnetic fields are discontinuous solutions to the Schrödinger equations, a

* Corresponding author. Tel.: +1 704 687 4581; fax: +1 704 687 6415.
E-mail address: wcai@uncc.edu (W. Cai).

0021-9991/$ - see front matter © 2008 Elsevier Inc. All rights reserved.
doi:10.1016/j.jcp.2008.03.044

property not shared by the probability wave functions of quantum mechanics. Since its introduction by Feit and Fleck in 1978 [1,2], the BPM has become a very popular method in the engineering communities for modeling optical waveguides. Different variants of the method, using various types of spatial discretization in the cross section of waveguides, have been proposed, such as the finite element (FE)-BPM [4], the fast Fourier transform (FFT)-BPM [5] and the finite difference (FD)-BPM [6]. However, discontinuities in fields across material interfaces have not been addressed so far, and as a result, large errors in numerical solutions may occur near the material interfaces due to large difference of dielectric constants.

As existing BPMs do not have the capability to treat discontinuities in the electromagnetic fields associated with wave propagations in inhomogeneous waveguides, it is our goal in this paper to develop a new BPM which will allow us to accurately handle those field discontinuities. To achieve this objective, we will apply a recently developed discontinuous Galerkin method – generalized discontinuous Galerkin (GDG) method [3] – designed specifically to compute discontinuous solutions of Schrödinger equations. The GDG method reformulates the Schrödinger equations by incorporating the jump conditions in the solutions and derivatives as Dirac δ-source terms on the material interface and treating the solutions to the Schrödinger equations as generalized functions (distributions). Discontinuous Galerkin projections are then applied to the reformulated partial differential equations for the generalized functions. In this paper, we will combine the GDG method and the traditional BPM for computing electromagnetic wave propagations in inhomogeneous optical waveguides. First, we derive the envelope function formulation as in the traditional BPM and recast the interface conditions of electromagnetic field components as jump conditions for the envelope functions for the field components. Those jump conditions are then incorporated into the Schrödinger equations for either the electric or magnetic components, for which the GDG–BPM will be constructed. Moreover, by using the Gauss laws for electric and magnetic fields, the equations for E_z or H_z components can be replaced by simple ordinary differential equations in time, thus reducing the computational costs by one third. In the end, four versions of the vectorial GDG–BPM are obtained where large jumps in the optical fields and/or their derivatives can be approximated accurately as demonstrated by various numerical tests.

The paper is organized as follows. In Section 2, we give the envelope formulation for the electromagnetic fields and derive the corresponding interface jump conditions. In Section 3, we present the GDG–BPM for the electric field, which employs the paraxial approximations and incorporates the jump conditions for the envelope functions. Section 4 follows similar procedure as in Section 3 for the magnetic field components. Section 5 describes the Galerkin discretization for the PDE systems obtained in Sections 3 and 4. Section 6 contains numerical studies of the convergence and comparison of the proposed four versions of the GDG–BPM and provides simulation results of various optical waveguides. Finally, Section 7 gives the conclusion of the paper.

2. Envelope functions for electromagnetic fields and interface jump conditions

In this section, we present the envelope function formulation used in BPMs for the electromagnetic fields. We also recast the interface conditions for the electromagnetic fields as jump conditions for the envelope functions. The explicit forms for the jump conditions will then be incorporated into the GDG method in next two sections.

Fig. 1 shows the cross section Ω of an optical waveguide with a core Ω_1, a cladding Ω_2 and an interface at $\Gamma = \Omega_1 \cap \Omega_2$ with an exterior normal direction $n = (n_x, n_y)$. As in a traditional BPM for optical waveguides, we assume that the electric or magnetic field takes the following envelope form, for instance:

$$\vec{E} = (E_x(x,y,z), E_y(x,y,z), E_z(x,y,z)) = (\varphi_1(x,y,z), \varphi_2(x,y,z), \varphi_3(x,y,z))\mathrm{e}^{-\mathrm{i}\beta z}, \quad \beta = \beta_l \quad \text{in } \Omega_l,\ l = 1,2 \tag{1}$$

for the electric field. The envelope functions φ_l are assumed to vary slowly along the *propagation direction* z, which will be denoted as the time variable t in the BPM [1,2].

Let us denote the jump of a function φ at the position τ along $n = (n_x, n_y)$ on Γ as

$$[\varphi(\tau,t)] := \varphi(\tau^+,t) - \varphi(\tau^-,t). \tag{2}$$

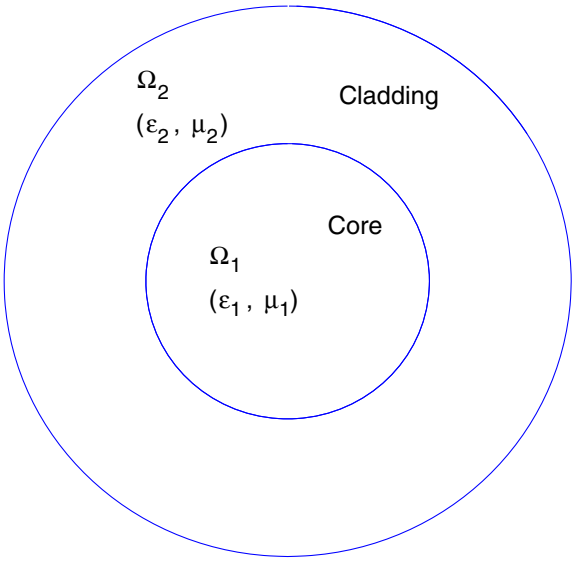

Fig. 1. Cross section of a cylindrical-core optical fiber.

Then, for any point (x^*, y^*) on the interface, for $I = 1, 2, 3$, the jump data

$$f_I(x^*, y^*, t) = [\varphi_I(x^*, y^*, t)] = \varphi_I(x^{*+}, y^{*+}, t) - \varphi_I(x^{*-}, y^{*-}, t),$$
$$g_I(x^*, y^*, t) = \left[\frac{\partial \varphi_I(x^*, y^*, t)}{\partial n}\right] = \frac{\partial \varphi_I(x^{*+}, y^{*+}, t)}{\partial n} - \frac{\partial \varphi_I(x^{*-}, y^{*-}, t)}{\partial n},$$

can be shown to satisfy identities based on the interface conditions for the electromagnetic fields and the Maxwell's equations as follows.

To derive the jump data f_I of the electric field, we start from the interface conditions of the electric field

$$\epsilon_1 E_\xi^- = \epsilon_2 E_\xi^+, \quad E_\eta^- = E_\eta^+, \quad E_z^- = E_z^+, \tag{3}$$

where ξ, η are the local normal and tangential coordinates on the interface Γ and $E_\xi = E_x n_x + E_y n_y$, $E_\eta = -E_x n_y + E_y n_x$ are the normal and the tangential electric field components, respectively. Using the envelope assumption of (1) and denoting

$$\varphi_\xi = \varphi_1 n_x + \varphi_2 n_y, \quad \varphi_\eta = -\varphi_1 n_y + \varphi_2 n_x, \quad \Delta\beta = \beta_1 - \beta_2, \tag{4}$$

$$\gamma_f = \frac{\epsilon_1}{\epsilon_2} e^{-i\Delta\beta t}, \tag{5}$$

we can get

$$\gamma_f \varphi_\xi^- = \varphi_\xi^+, \quad e^{-i\Delta\beta t}\varphi_\eta^- = \varphi_\eta^+, \quad e^{-i\Delta\beta t}\varphi_3^- = \varphi_3^+. \tag{6}$$

From (6), f_I can be written in terms of $(\varphi_\xi^-,\ \varphi_\eta^-,\ \varphi_3^-)$ and $(\varphi_\xi^+,\ \varphi_\eta^+,\ \varphi_3^+)$ in a symmetric form

$$\begin{cases} \begin{pmatrix} f_1 \\ f_2 \end{pmatrix} = \frac{1}{2}\begin{bmatrix} n_x & -n_y \\ n_y & n_x \end{bmatrix} \begin{pmatrix} (\gamma_f - 1)\varphi_\xi^- + (1 - \gamma_f^{-1})\varphi_\xi^+ \\ (e^{-i\Delta\beta t} - 1)\varphi_\eta^- + (1 - e^{i\Delta\beta t})\varphi_\eta^+ \end{pmatrix}, \\ f_3 = \frac{1}{2}[(e^{-i\Delta\beta t} - 1)\varphi_3^- + (1 - e^{i\Delta\beta t})\varphi_3^+], \end{cases} \tag{7}$$

which expresses the interface conditions (3) of the electric field in terms of the envelope functions.

To derive the jump data g_I for the normal derivative of the electric field, we consider the interface conditions of the magnetic field

$$\mu_1 H_\xi^- = \mu_2 H_\xi^+, \quad H_\eta^- = H_\eta^+, \quad H_z^- = H_z^+. \tag{8}$$

With the envelope assumption (1) and the Ampere's law

$$\nabla \times \vec{E} = -\mathrm{i}\omega\mu\vec{H}, \tag{9}$$

defining

$$\gamma_g = \frac{\mu_2}{\mu_1}\mathrm{e}^{-\mathrm{i}\Delta\beta t}, \tag{10}$$

we get

$$\begin{cases} \mathrm{e}^{-\mathrm{i}\Delta\beta t}\left(\frac{\partial\varphi_3}{\partial\eta} - \left(\frac{\partial\varphi_\eta}{\partial t} - \mathrm{i}\beta_1\varphi_\eta\right)\right)^- = \left(\frac{\partial\varphi_3}{\partial\eta} - \left(\frac{\partial\varphi_\eta}{\partial t} - \mathrm{i}\beta_2\varphi_\eta\right)\right)^+, \\ \gamma_g\left(\left(\frac{\partial\varphi_\xi}{\partial t} - \mathrm{i}\beta_1\varphi_\xi\right) - \frac{\partial\varphi_3}{\partial\xi}\right)^- = \left(\left(\frac{\partial\varphi_\xi}{\partial t} - \mathrm{i}\beta_2\varphi_\xi\right) - \frac{\partial\varphi_3}{\partial\xi}\right)^+, \\ \gamma_g\left(\frac{\partial\varphi_\eta}{\partial\xi} - \frac{\partial\varphi_\xi}{\partial\eta}\right)^- = \left(\frac{\partial\varphi_\eta}{\partial\xi} - \frac{\partial\varphi_\xi}{\partial\eta}\right)^+. \end{cases} \tag{11}$$

From the second equation, g_3 can be expressed in terms of $\frac{\partial\varphi_3^-}{\partial\xi}$ and $\frac{\partial\varphi_3^+}{\partial\xi}$ in a symmetric form as

$$g_3 = \frac{1}{2}\left[(1+\gamma_g^{-1})\left(\frac{\partial\varphi_\xi^+}{\partial t} - \mathrm{i}\beta_2\varphi_\xi^+\right) + (\gamma_g - 1)\frac{\partial\varphi_3^-}{\partial\xi} - (1+\gamma_g)\left(\frac{\partial\varphi_\xi^-}{\partial t} - \mathrm{i}\beta_1\varphi_\xi^-\right) + (1-\gamma_g^{-1})\frac{\partial\varphi_3^+}{\partial\xi}\right]. \tag{12}$$

The right-hand side of (12) actually involves time derivatives of φ_1, φ_2 on both sides of the interface, which can be replaced with spatial derivatives by using the time dependent Schrödinger equations for φ_1, φ_2 in Section 3 (electric field) and Section 4 (magnetic field), respectively.

Next, using the identity

$$n_x g_1 + n_y g_2 = \frac{\partial\varphi_\xi^+}{\partial\xi} - \frac{\partial\varphi_\xi^-}{\partial\xi} \tag{13}$$

and the third equation in (11), after some manipulations, we find g_1 and g_2 in terms of $\left(\frac{\partial\varphi_\xi^-}{\partial\xi}, \frac{\partial\varphi_\eta^-}{\partial\xi}\right)$ and $\left(\frac{\partial\varphi_\xi^+}{\partial\xi}, \frac{\partial\varphi_\eta^+}{\partial\xi}\right)$ in a symmetric form

$$\begin{pmatrix} g_1 \\ g_2 \end{pmatrix} = \frac{1}{2}\begin{bmatrix} n_x & -n_y \\ n_y & n_x \end{bmatrix}\begin{pmatrix} 2\frac{\partial\varphi_\xi^+}{\partial\xi} - 2\frac{\partial\varphi_\xi^-}{\partial\xi} \\ (\gamma_g - 1)\frac{\partial\varphi_\eta^-}{\partial\xi} + \left(1 - \frac{1}{\gamma_g}\right)\frac{\partial\varphi_\eta^+}{\partial\xi} + \left(1 + \frac{1}{\gamma_g}\right)\frac{\partial\varphi_\xi^+}{\partial\eta} - (1+\gamma_g)\frac{\partial\varphi_\xi^-}{\partial\eta} \end{pmatrix}. \tag{14}$$

Similarly, the jump data f_I for the magnetic field components and g_I for their normal derivatives can be shown to satisfy (7), (12) and (14) with

$$\gamma_f = \frac{\mu_1}{\mu_2}\mathrm{e}^{-\mathrm{i}\Delta\beta t}, \quad \gamma_g = \frac{\epsilon_2}{\epsilon_1}\mathrm{e}^{-\mathrm{i}\Delta\beta t}. \tag{15}$$

3. GDG–BPM formulation for the electric field

In this section, we combine the GDG [3] with the BPM to obtain a full vectorial GDG–BPM for optical waveguides where the electromagnetic fields and/or their derivatives can be discontinuous across material interfaces. To illustrate the GDG–BPM, we consider the paraxial approximation of a standard cylindrical optical fiber (Fig. 1).

Assuming that the field is time harmonic with a frequency ω and there is no charge nor current sources, we can derive the vector wave equation for $\vec{E}(x, y, z = t)$ components as

$$\nabla \times \nabla \times \vec{E} = \omega^2\epsilon\mu\vec{E}, \tag{16}$$

which will leads to

$$\nabla^2\vec{E} + \omega^2\epsilon\mu\vec{E} = \nabla(\nabla \cdot \vec{E}). \tag{17}$$

Since $\nabla \cdot (\epsilon\vec{E}) = 0$, we have

$$\nabla \cdot \vec{E} = \nabla \cdot \left(\frac{1}{\epsilon}\epsilon\vec{E}\right) = -\frac{1}{\epsilon}(\nabla\epsilon \cdot \overrightarrow{E}) = -\nabla\hat{\epsilon} \cdot \vec{E}, \tag{18}$$

where $\hat{\epsilon} \equiv \ln \epsilon$. Assuming that $\epsilon = \epsilon(x, y)$ is uniform along the propagation direction, the vector Helmholtz equation (17) becomes

$$\nabla^2 \vec{E} + \omega^2 \epsilon \mu \vec{E} = -\nabla \left(\frac{\partial \hat{\epsilon}}{\partial x} E_x + \frac{\partial \hat{\epsilon}}{\partial y} E_y \right). \tag{19}$$

Based on the slow envelope assumption in (1) (paraxial approximation [7]), i.e.

$$\left| \frac{\partial^2 \varphi_I}{\partial t^2} \right| \ll 2\beta \left| \frac{\partial \varphi_I}{\partial t} \right|, \quad I = 1, 2, 3, \tag{20}$$

we ignore the second order derivative in t and obtain the following coupled equations at $(x, y) \notin \Gamma$:

$$\mathrm{i}2\beta \frac{\partial \varphi_1}{\partial t} = \frac{\partial^2 \varphi_1}{\partial x^2} + \frac{\partial^2 \varphi_1}{\partial y^2} + (\omega^2 \epsilon \mu - \beta^2)\varphi_1 + \frac{\partial^2 \hat{\epsilon}}{\partial x^2} \varphi_1 + \frac{\partial^2 \hat{\epsilon}}{\partial x \partial y} \varphi_2 + \frac{\partial \hat{\epsilon}}{\partial x} \frac{\partial \varphi_1}{\partial x} + \frac{\partial \hat{\epsilon}}{\partial y} \frac{\partial \varphi_2}{\partial x}, \tag{21a}$$

$$\mathrm{i}2\beta \frac{\partial \varphi_2}{\partial t} = \frac{\partial^2 \varphi_2}{\partial x^2} + \frac{\partial^2 \varphi_2}{\partial y^2} + (\omega^2 \epsilon \mu - \beta^2)\varphi_2 + \frac{\partial^2 \hat{\epsilon}}{\partial x \partial y} \varphi_1 + \frac{\partial^2 \hat{\epsilon}}{\partial y^2} \varphi_2 + \frac{\partial \hat{\epsilon}}{\partial x} \frac{\partial \varphi_1}{\partial y} + \frac{\partial \hat{\epsilon}}{\partial y} \frac{\partial \varphi_2}{\partial y}, \tag{21b}$$

$$\mathrm{i}2\beta \frac{\partial \varphi_3}{\partial t} = \frac{\partial^2 \varphi_3}{\partial x^2} + \frac{\partial^2 \varphi_3}{\partial y^2} + (\omega^2 \epsilon \mu - \beta^2)\varphi_3 + \frac{\partial \hat{\epsilon}}{\partial x} \left(\frac{\partial \varphi_1}{\partial t} - \mathrm{i}\beta \varphi_1 \right) + \frac{\partial \hat{\epsilon}}{\partial y} \left(\frac{\partial \varphi_2}{\partial t} - \mathrm{i}\beta \varphi_2 \right), \tag{21c}$$

where $\beta = \beta_l$ in $\Omega_l, l = 1, 2$.

For convenience, we define the jump data for the dielectric constant ϵ as

$$f_{\hat{\epsilon}}(x^*, y^*, t) = [\hat{\epsilon}(x^*, y^*, t)] = \hat{\epsilon}(x^{*+}, y^{*+}, t) - \hat{\epsilon}(x^{*-}, y^{*-}, t),$$
$$g_{\hat{\epsilon}}(x^*, y^*, t) = \left[\frac{\partial \hat{\epsilon}(x^*, y^*, t)}{\partial n} \right] = \frac{\partial \hat{\epsilon}(x^{*+}, y^{*+}, t)}{\partial n} - \frac{\partial \hat{\epsilon}(x^{*-}, y^{*-}, t)}{\partial n}.$$

Following the procedure proposed in [3], we can rewrite the system (21a)–(21c) using Dirac δ functions as

Formulation A: For $I = 1, 2, 3$

$$\mathrm{i}2\beta \frac{\partial \varphi_I}{\partial t} = \frac{\partial p_I}{\partial x} + \frac{\partial q_I}{\partial y} - \delta(\xi - \xi^*)|\nabla \xi|^2 g_I + S_I, \tag{22a}$$

$$p_I = \frac{\partial \varphi_I}{\partial x} - \delta(\xi - \xi^*) f_I \frac{\partial \xi}{\partial x}, \tag{22b}$$

$$q_I = \frac{\partial \varphi_I}{\partial y} - \delta(\xi - \xi^*) f_I \frac{\partial \xi}{\partial y}, \tag{22c}$$

where $\beta = \beta_l$ in $\Omega_l, l = 1, 2$ and the jump data f_I, g_I are given by (7), (12), (14) with (5), (10) to enforce the physical jump conditions for the electromagnetic field components. And, the lower order terms above are

$$S_1(\varphi_1, \varphi_2, p_1, p_2) = (\omega^2 \epsilon \mu - \beta^2)\varphi_1 + p_{\hat{\epsilon}}^x \varphi_1 + q_{\hat{\epsilon}}^x \varphi_2 + p_{\hat{\epsilon}} p_1 + q_{\hat{\epsilon}} p_2,$$
$$S_2(\varphi_1, \varphi_2, q_1, q_2) = (\omega^2 \epsilon \mu - \beta^2)\varphi_2 + p_{\hat{\epsilon}}^y \varphi_1 + q_{\hat{\epsilon}}^y \varphi_2 + p_{\hat{\epsilon}} q_1 + q_{\hat{\epsilon}} q_2,$$
$$S_3(\varphi_1, \varphi_2, \varphi_3) = (\omega^2 \epsilon \mu - \beta^2)\varphi_3 + p_{\hat{\epsilon}} \left(\frac{\partial \varphi_1}{\partial t} - \mathrm{i}\beta \varphi_1 \right) + q_{\hat{\epsilon}} \left(\frac{\partial \varphi_2}{\partial t} - \mathrm{i}\beta \varphi_2 \right),$$

where $\frac{\partial \varphi_1}{\partial t}$ and $\frac{\partial \varphi_2}{\partial t}$ in S_3 can be replaced by (22a) with $I = 1, 2$ and

$$p_{\hat{\epsilon}} = \frac{\partial \hat{\epsilon}}{\partial x} - \delta(\xi - \xi^*) f_{\hat{\epsilon}} \frac{\partial \xi}{\partial x}, \quad q_{\hat{\epsilon}} = \frac{\partial \hat{\epsilon}}{\partial y} - \delta(\xi - \xi^*) f_{\hat{\epsilon}} \frac{\partial \xi}{\partial y}, \quad p_{\hat{\epsilon}}^x = \frac{\partial p_{\hat{\epsilon}}}{\partial x} - \delta(\xi - \xi^*) \left(\frac{\partial f_{\hat{\epsilon}}}{\partial x} + g_{\hat{\epsilon}} \frac{\partial \xi}{\partial x} \right) \frac{\partial \xi}{\partial x},$$
$$p_{\hat{\epsilon}}^y = \frac{\partial p_{\hat{\epsilon}}}{\partial y} - \delta(\xi - \xi^*) \left(\frac{\partial f_{\hat{\epsilon}}}{\partial x} + g_{\hat{\epsilon}} \frac{\partial \xi}{\partial x} \right) \frac{\partial \xi}{\partial y}, \quad q_{\hat{\epsilon}}^x = \frac{\partial p_{\hat{\epsilon}}}{\partial x} - \delta(\xi - \xi^*) \left(\frac{\partial f_{\hat{\epsilon}}}{\partial y} + g_{\hat{\epsilon}} \frac{\partial \xi}{\partial y} \right) \frac{\partial \xi}{\partial x},$$
$$q_{\hat{\epsilon}}^y = \frac{\partial p_{\hat{\epsilon}}}{\partial y} - \delta(\xi - \xi^*) \left(\frac{\partial f_{\hat{\epsilon}}}{\partial y} + g_{\hat{\epsilon}} \frac{\partial \xi}{\partial y} \right) \frac{\partial \xi}{\partial y}.$$

Here, $p_{\hat{\epsilon}}, q_{\hat{\epsilon}}, p_{\hat{\epsilon}}^x, p_{\hat{\epsilon}}^y, q_{\hat{\epsilon}}^x, q_{\hat{\epsilon}}^y$ will be zero if ϵ is a piecewise constant.

Remark 1. In the above derivations, partial derivatives of $f(x,y)$ on Γ are used while the data $f(x,y)$ is only given on the interface Γ. Therefore, some types of smooth extension away from the interface will be needed to yield those partial derivatives. The simplest one, which we use, is to use a constant extension locally along the normal direction of the interface Γ, i.e., assuming $\frac{\partial f}{\partial \xi} = 0$. Then, we have

$$\frac{\partial f}{\partial x} = \frac{\partial f}{\partial \xi}\frac{\partial \xi}{\partial x} + \frac{\partial f}{\partial \eta}\frac{\partial \eta}{\partial x} = \frac{\partial f}{\partial \eta}\frac{\partial \eta}{\partial x}, \quad \frac{\partial f}{\partial y} = \frac{\partial f}{\partial \xi}\frac{\partial \xi}{\partial y} + \frac{\partial f}{\partial \eta}\frac{\partial \eta}{\partial y} = \frac{\partial f}{\partial \eta}\frac{\partial \eta}{\partial y}. \tag{23}$$

The extension is by no means unique. However, the accuracy of the resulting numerical methods will not be affected by a specific choice of the extension as long as the extension produces a locally smooth function.

Remark 2. As φ, p, q are considered piecewise continuous functions over Ω, $\frac{\partial \varphi}{\partial x}, \frac{\partial p}{\partial x}$ will be treated as distributions or generalized functions [8]. The key idea here is the usage of the δ source terms to compensate the singularity introduced by the (time dependent) jump conditions at the interface. Those δ-functions act as penalty terms in the "collocation" sense to enforce the solution jump conditions. In contrast, the traditional interior penalty method [9–14] uses Lagrange multipliers to enforce the "continuity" of the solutions.

Alternatively, we can use the Gauss law $\nabla \cdot (\epsilon E) = 0$ to solve for the E_z component, which results in the following equation for $\varphi_3(x,y,z := t)$:

$$\epsilon\frac{\partial \varphi_3}{\partial t} = -\epsilon\frac{\partial \varphi_1}{\partial x} - \epsilon\frac{\partial \varphi_2}{\partial y} - \epsilon_x\varphi_1 - \epsilon_y\varphi_2 - (\epsilon_t - \mathrm{i}\beta\epsilon)\varphi_3. \tag{24}$$

If the evolution Eq. (24) is used for φ_3, instead of (22a)–(22c), we will have the following alternative version of the GDG–BPM for the electric field.

Formulation B: For $I = 1, 2$,

$$\mathrm{i}2\beta\frac{\partial \varphi_I}{\partial t} = \frac{\partial p_I}{\partial x} + \frac{\partial q_I}{\partial y} - \delta(\xi - \xi^*)|\nabla\xi|^2 g_I + S_I, \tag{25a}$$

$$\epsilon\frac{\partial \varphi_3}{\partial t} = -\epsilon p_1 - \epsilon q_2 - \epsilon_x\varphi_1 - \epsilon_y\varphi_2 - (\epsilon_t - \mathrm{i}\beta\epsilon)\varphi_3, \tag{25b}$$

$$p_I = \frac{\partial \varphi_I}{\partial x} - \delta(\xi - \xi^*)f_I\frac{\partial \xi}{\partial x}, \tag{25c}$$

$$q_I = \frac{\partial \varphi_I}{\partial y} - \delta(\xi - \xi^*)f_I\frac{\partial \xi}{\partial y}, \tag{25d}$$

where $\beta = \beta_l$ in Ω_l, $l = 1, 2$.

The time evolution equation for φ_3 in *Formulation B* is a simple ODE, thus requiring less computational cost compared to the corresponding equation for φ_3 in *Formulation A*.

4. GDG–BPM formulation for the magnetic field

Similarly, we can get a vector wave equation for $\vec{H}$ components as

$$\nabla \times \left(\frac{1}{\epsilon}\nabla \times \vec{H}\right) = \omega^2\mu\vec{H}. \tag{26}$$

Assuming that μ is a constant (implying $\nabla \cdot \vec{H} = 0$), we get

$$\nabla \times \left(\frac{1}{\epsilon}\nabla \times \vec{H}\right) = -\frac{1}{\epsilon}\nabla^2\vec{H} + \left(\nabla\frac{1}{\epsilon}\right) \times (\nabla \times \vec{H}). \tag{27}$$

Therefore, we have

$$\frac{1}{\epsilon}\nabla^2\vec{H} = \nabla\frac{1}{\epsilon} \times (\nabla \times \vec{H}) - \omega^2\mu\vec{H}. \tag{28}$$

Again, we assume $\vec{H}$ has an envelope formulation as

$$\vec{H} = (H_x(x,y,z), H_y(x,y,z), H_z(x,y,z)) = (\varphi_1(x,y,z), \varphi_2(x,y,z), \varphi_3(x,y,z))\mathrm{e}^{-\mathrm{i}\beta z}, \quad \beta = \beta_l \text{ in } \Omega_l, \ l = 1,2. \tag{29}$$

Then, by dropping the term $\frac{\partial^2 \varphi_l}{\partial z^2}$ based on the paraxial approximation, replacing z by t and assuming that $\hat{\epsilon} \equiv \ln \epsilon$ is independent of z, we get the following coupled equations at $(x,y) \notin \Gamma$:

$$\mathrm{i}2\beta \frac{\partial \varphi_1}{\partial t} = \frac{\partial^2 \varphi_1}{\partial x^2} + \frac{\partial^2 \varphi_1}{\partial y^2} + (\omega^2 \epsilon\mu - \beta^2)\varphi_1 + \frac{\partial \hat{\epsilon}}{\partial y}\left(\frac{\partial \varphi_2}{\partial x} - \frac{\partial \varphi_1}{\partial y}\right), \tag{30a}$$

$$\mathrm{i}2\beta \frac{\partial \varphi_2}{\partial t} = \frac{\partial^2 \varphi_2}{\partial x^2} + \frac{\partial^2 \varphi_2}{\partial y^2} + (\omega^2 \epsilon\mu - \beta^2)\varphi_2 - \frac{\partial \hat{\epsilon}}{\partial x}\left(\frac{\partial \varphi_2}{\partial x} - \frac{\partial \varphi_1}{\partial y}\right), \tag{30b}$$

$$\mathrm{i}2\beta \frac{\partial \varphi_3}{\partial t} = \frac{\partial^2 \varphi_3}{\partial x^2} + \frac{\partial^2 \varphi_3}{\partial y^2} + (\omega^2 \epsilon\mu - \beta^2)\varphi_3 + \frac{\partial \hat{\epsilon}}{\partial x}\left(\frac{\partial \varphi_1}{\partial t} - \mathrm{i}\beta\varphi_1 - \frac{\partial \varphi_3}{\partial x}\right) + \frac{\partial \hat{\epsilon}}{\partial y}\left(\frac{\partial \varphi_2}{\partial t} - \mathrm{i}\beta\varphi_2 - \frac{\partial \varphi_3}{\partial y}\right), \tag{30c}$$

where $\beta = \beta_l$ in $\Omega_l, l = 1,2$.

For the interface conditions, similar to the previous section, we use f_l and g_l to denote the jumps of φ_l and $\frac{\partial \varphi_l}{\partial n}$ on the interface, respectively.

Now, we use the δ-function and auxiliary variables p and q to rewrite (30a)–(30c) as

Formulation C: For $I = 1,2,3$,

$$\mathrm{i}2\beta \frac{\partial \varphi_I}{\partial t} = \frac{\partial p_I}{\partial x} + \frac{\partial q_I}{\partial y} - \delta(\xi - \xi^*)|\nabla \xi|^2 g_I + S_I, \tag{31a}$$

$$p_I = \frac{\partial \varphi_I}{\partial x} - \delta(\xi - \xi^*) f_I \frac{\partial \xi}{\partial x}, \tag{31b}$$

$$q_I = \frac{\partial \varphi_I}{\partial y} - \delta(\xi - \xi^*) f_I \frac{\partial \xi}{\partial y}, \tag{31c}$$

where $\beta = \beta_l$ in $\Omega_l, l = 1,2$, and the jump data f_I, g_I again are given by (7), (12), (14) with (15) to enforce the physical interface conditions for the electromagnetic field components. The lower order source terms are given as

$$\begin{aligned}
&S_1(\varphi_1, \varphi_2, p_2, q_1) = (\omega^2 \epsilon\mu - \beta^2)\varphi_1 + q_{\hat{\epsilon}}(p_2 - q_1),\\
&S_2(\varphi_1, \varphi_2, p_2, q_1) = (\omega^2 \epsilon\mu - \beta^2)\varphi_2 - p_{\hat{\epsilon}}(p_2 - q_1),\\
&S_3(\varphi_1, \varphi_2, \varphi_3, p_3, q_3) = (\omega^2 \epsilon\mu - \beta^2)\varphi_3 + p_{\hat{\epsilon}}\left(\frac{\partial \varphi_1}{\partial t} - \mathrm{i}\beta\varphi_1 - p_3\right) + q_{\hat{\epsilon}}\left(\frac{\partial \varphi_2}{\partial t} - \mathrm{i}\beta\varphi_2 - q_3\right),
\end{aligned}$$

where $\frac{\partial \varphi_1}{\partial t}$ and $\frac{\partial \varphi_2}{\partial t}$ in S_3 can be replaced by (31a) and

$$p_{\hat{\epsilon}} = \frac{\partial \hat{\epsilon}}{\partial x} - \delta(\xi - \xi^*) f_{\hat{\epsilon}} \frac{\partial \xi}{\partial x}, \quad q_{\hat{\epsilon}} = \frac{\partial \hat{\epsilon}}{\partial y} - \delta(\xi - \xi^*) f_{\hat{\epsilon}} \frac{\partial \xi}{\partial y}.$$

$p_{\hat{\epsilon}}, q_{\hat{\epsilon}}$ will be zero if ϵ is a piecewise constant.

Similarly, we can solve the H_z component in terms of H_x and H_y using $\nabla \cdot H = 0$ and obtain

$$\frac{\partial \varphi_3}{\partial t} = -\frac{\partial \varphi_1}{\partial x} - \frac{\partial \varphi_2}{\partial y} + \mathrm{i}\beta\varphi_3. \tag{32}$$

As a result, we have the following alternative formulation for the magnetic field.

Formulation D: For $I = 1,2$,

$$\mathrm{i}2\beta \frac{\partial \varphi_I}{\partial t} = \frac{\partial p_I}{\partial x} + \frac{\partial q_I}{\partial y} - \delta(\xi - \xi^*)|\nabla \xi|^2 g_I + S_I, \tag{33a}$$

$$\frac{\partial \varphi_3}{\partial t} = -p_1 - q_2 + \mathrm{i}\beta\varphi_3, \tag{33b}$$

$$p_I = \frac{\partial \varphi_I}{\partial x} - \delta(\xi - \xi^*) f_I \frac{\partial \xi}{\partial x}, \tag{33c}$$

$$q_I = \frac{\partial \varphi_I}{\partial y} - \delta(\xi - \xi^*) f_I \frac{\partial \xi}{\partial y}, \tag{33d}$$

where $\beta = \beta_l$ in $\Omega_l, l = 1, 2$.

Again, the time evolution equation for φ_3 in *Formulation D* is a simple ODE, thus requiring less computational cost compared with the corresponding equation for φ_3 in *Formulation C*.

5. Discontinuous Galerkin discretization

In this section, we present the procedure of discontinuous Galerkin projection [15] based on *Formulation A* (22a)–(22c) while the same procedure can be applied to *Formulations B–D*.

For each element K in the discretization of Ω, let $P^J(K)$ denote the space of polynomials in K of degree at most J and $v \in L^1(\Omega)$ be a test function, where $v|_K \in P^J(K)$. Multiplying the Eqs. (22a)–(22c) by the test function $v(x, y)$ and integrating by parts in K, we get

$$\mathrm{i}2\beta \int_K \frac{\partial \varphi_I}{\partial t} v \,\mathrm{d}x\mathrm{d}y = \int_{\partial K} h^x_{\varphi_I} v n_x \,\mathrm{d}s - \int_K p_I \frac{\partial v}{\partial x} \,\mathrm{d}x\,\mathrm{d}y + \int_{\partial K} h^y_{\varphi_I} v n_y \,\mathrm{d}s - \int_K q_I \frac{\partial v}{\partial y} \,\mathrm{d}x\,\mathrm{d}y + \int_K S_I v \,\mathrm{d}x\,\mathrm{d}y, \tag{34a}$$

$$\int_K p_I v \,\mathrm{d}x\,\mathrm{d}y = \int_{\partial K} h_{p_I} v n_x \,\mathrm{d}s - \int_K \varphi_I \frac{\partial v}{\partial x} \,\mathrm{d}x\,\mathrm{d}y, \tag{34b}$$

$$\int_K q_I v \,\mathrm{d}x\,\mathrm{d}y = \int_{\partial K} h_{q_I} v n_y \mathrm{d}s - \int_K \varphi_I \frac{\partial v}{\partial y} \,\mathrm{d}x\,\mathrm{d}y, \tag{34c}$$

where $(h^x_{\varphi_I}, h^y_{\varphi_I}, h_{p_I} = h_{q_I})$ are numerical fluxes, which approximate (p_I, q_I, φ_I) at ∂K. For $\vec{x} = (x, y) \in \partial K$

$$h^x_{\varphi_I}(\vec{x}^{\pm}) = \{p_I\} \pm a^x_I, h^y_{\varphi_I}(\vec{x}^{\pm}) = \{q_I\} \pm a^y_I, h_{p_I}(\vec{x}^{\pm}) = \{\varphi_I\} \pm b_I, \tag{35}$$

where a^x_I, a^y_I, b_I are defined as

$$(a^x_I,\ a^y_I,\ b_I) = \begin{cases} \left(\frac{1}{2} g_I |\nabla \xi| n_x, \frac{1}{2} g_I |\nabla \xi| n_y, \frac{1}{2} f_I\right), & \text{if } \Gamma \cap K \neq \emptyset \\ (0, 0, 0), & \text{if } \Gamma \cap K = \emptyset \end{cases}. \tag{36}$$

In the definition of the numerical fluxes (35), simple averages are used for all element edges of K except the edge coinciding with the material interface Γ where average plus/minus half of the jumps will be used. The definition and derivation of the fluxes in (34a)–(34c) can be found in [3].

Let $\phi_j(x, y)$, $j = 0, 1, \ldots, n_J$ be the basis functions, where $n_J + 1$ is the number of basis functions required for a Jth order approximation. By expanding φ_I, p_I, q_I as

$$\varphi_I = \sum_{j=0}^{n_J} \varphi_{I,j}(t)\phi_j(x, y), \quad q_I = \sum_{j=0}^{n_J} q_{I,j}(t)\phi_j(x, y), \quad p_I = \sum_{j=0}^{n_J} p_{I,j}(t)\phi_j(x, y) \tag{37}$$

and choosing the test function $v(x, y) = \phi_l(x, y)$ for $l = 0, 1, \ldots, n_J$, we get

$$\mathrm{i}2\beta \sum_j m_{lj} \frac{\mathrm{d}\varphi_{I,j}}{\mathrm{d}t} = \int_{\partial K} (h^x_{\varphi_I} n_x + h^y_{\varphi_I} n_y)\phi_l \,\mathrm{d}s - \sum_j (m^x_{lj} p_{I,j} + m^y_{lj} q_{I,j} + s_{I,l}), \tag{38a}$$

$$\sum_j m_{lj} p_{I,j} = \int_{\partial K} h_{p_I} n_x \phi_l \,\mathrm{d}s - \sum_j m^x_{lj} \varphi_{I,j}, \tag{38b}$$

$$\sum_j m_{lj} q_{I,j} = \int_{\partial K} h_{q_I} n_y \phi_l \,\mathrm{d}s - \sum_j m^y_{lj} \varphi_{I,j}, \tag{38c}$$

where $s_{I,l} = \int_K S_I \phi_l \,\mathrm{d}x\,\mathrm{d}y$ and

$$m_{lj} = \int_K \phi_l \phi_j \,\mathrm{d}x\,\mathrm{d}y, \quad m^x_{lj} = \int_K \frac{\partial \phi_l}{\partial x} \phi_j \,\mathrm{d}x\,\mathrm{d}y, \quad m^y_{lj} = \int_K \frac{\partial \phi_l}{\partial y} \phi_j \,\mathrm{d}x\,\mathrm{d}y. \tag{39}$$

We define a mass matrix M and two stiff matrices M^x, M^y as

$$M = (m_{i+1,j+1}), \quad M^x = (m^x_{i+1,j+1}), \quad M^y = (m^y_{i+1,j+1}) \tag{40}$$

and vectors, for $I = 1, 2, 3$,

$$\vec{\varphi}_I = [\varphi_{I,0}, \ldots, \varphi_{I,n_J}]^{\mathrm{T}}, \quad \vec{\phi} = [\phi_0, \ldots, \phi_{n_J}]^{\mathrm{T}}, \quad \vec{p}_I = [p_{I,0}, \ldots, p_{I,n_J}]^{\mathrm{T}},$$
$$\vec{q}_I = [q_{I,0}, \ldots, q_{I,n_J}]^{\mathrm{T}}, \quad \vec{s}_I = [s_{I,0}, \ldots, s_{I,n_J}]^{\mathrm{T}}.$$

The following system of ODEs is obtained in each K for $I = 1, 2, 3$:

$$\mathrm{i}2\beta \frac{\mathrm{d}\vec{\varphi}_I}{\mathrm{d}t} = M^{-1}\left(\int_{\partial K} (h^x_{\varphi_I} n_x + h^y_{\varphi_I} n_y)\vec{\phi}\,\mathrm{d}s - M^x \vec{p}_I - M^y \vec{q}_I - \overrightarrow{s_I}\right), \tag{41}$$

$$\vec{p}_I = M^{-1}\left(\int_{\partial K} h_{p_I} n_x \vec{\phi}\,\mathrm{d}s - M^x \vec{\varphi}_I\right), \tag{42}$$

$$\vec{q}_I = M^{-1}\left(\int_{\partial K} h_{q_I} n_y \vec{\phi}\,\mathrm{d}s - M^y \vec{\varphi}_I\right). \tag{43}$$

Remark 3. Formulations A–D can all be written for the primary variable $\vec{\varphi}$, after eliminating the auxiliary variables p and q, in the form of

$$\frac{\mathrm{d}\vec{\varphi}}{\mathrm{d}t} = L\vec{\varphi}, \tag{44}$$

where L is the discretization matrix for the variable $\vec{\varphi}$.

6. Numerical results

In the following numerical tests, the time derivatives are discretized with a fourth order Runge–Kutta method and the time step Δt is estimated based on an empirical formula $\Delta t \leqslant (\Delta x)^2(2J+1)^2/\lambda_{\max}$ where Δx is the element size and $\lambda_{\max}$ is the largest magnitude of the eigenvalues of the matrix L in (44). All the results are reported after propagation for a 1 cm distance unless specified otherwise. In all the numerical simulations, we choose $\beta_1 = \beta_2 = \beta^*$, where β^* is the propagation constant. In Sections 6.1 and 6.2, exact boundary condition is used. Meanwhile, in Sections 6.3 and 6.4, as there is no exact solutions, standard transparent boundary condition (TBC) [16] is applied.

6.1. Propagation of LP01 modes using the electric field

In this section, we test the GDG–BPM on the LP01 mode in a cylindrical fiber (Fig. 1) with

$$\Omega_1 = \{(x,y)|x^2 + y^2 \leqslant r_0\}, \quad \Omega_2 = \{(x,y)|r_0 \leqslant x^2 + y^2 \leqslant R\}. \tag{45}$$

Denoting $J_n(r)$ – the nth order Bessel function of the first kind and $K_n(r)$ – the nth order modified Bessel function of the second kind, then, the LP01 mode for the electric components is given by

$$\varphi_1(x,y,t) = \begin{cases} -\left[\frac{1-s}{2}J_0\left(\frac{\alpha_1}{r_0}r\right)\cos(\Theta) - \frac{1+s}{2}J_2\left(\frac{\alpha_1}{r_0}r\right)\cos(2\theta+\Theta)\right]F_1(t), & \text{in} \quad \Omega_1, \\ -\left[\frac{1-s}{2}K_0\left(\frac{\alpha_2}{r_0}r\right)\cos(\Theta) + \frac{1+s}{2}K_2\left(\frac{\alpha_2}{r_0}r\right)\cos(2\theta+\Theta)\right]F_2(t), & \text{in} \quad \Omega_2, \end{cases}$$

$$\varphi_2(x,y,t) = \begin{cases} \left[\frac{1-s}{2}J_0\left(\frac{\alpha_1}{r_0}r\right)\sin(\Theta) + \frac{1+s}{2}J_2\left(\frac{\alpha_1}{r_0}r\right)\sin(2\theta+\Theta)\right]F_1(t), & \text{in} \quad \Omega_1, \\ \left[\frac{1-s}{2}K_0\left(\frac{\alpha_2}{r_0}r\right)\sin(\Theta) - \frac{1+s}{2}K_2\left(\frac{\alpha_2}{r_0}r\right)\sin(2\theta+\Theta)\right]F_2(t), & \text{in} \quad \Omega_2, \end{cases}$$

$$\varphi_3(x,y,t) = \begin{cases} \left(\mathrm{i}\beta^*\frac{r_0}{\alpha_1}\right)^{-1} J_1\left(\frac{\alpha_1}{r_0}r\right)\cos(\theta+\Theta)F_1(t), & \text{in} \quad \Omega_1, \\ \left(\mathrm{i}\beta^*\frac{r_0}{\alpha_2}\right)^{-1} K_1\left(\frac{\alpha_2}{r_0}r\right)\cos(\theta+\Theta)F_2(t), & \text{in} \quad \Omega_2, \end{cases}$$

where the time dependent factors $F_1(t)$ and $F_2(t)$ and three parameters s, α_1, α_2 are given as

$$F_1(t) = \mathrm{i}\beta^* \frac{r_0}{\alpha_1} \mathrm{e}^{\mathrm{i}(\beta_1 - \beta^*)t}, \quad F_2(t) = \mathrm{i}\beta^* \frac{r_0}{\alpha_2} \frac{J_1(\alpha_1)}{K_1(\alpha_2)} \mathrm{e}^{\mathrm{i}(\beta_2 - \beta^*)t}, \tag{46}$$

$$s = -1 + \frac{\alpha_1^2 \alpha_2^2}{\alpha_1^2 + \alpha_2^2} \frac{J_0(\alpha_1)}{\alpha_1 J_1(\alpha_1)} * \left(1 - \frac{\epsilon_2}{\epsilon_1}\right), \tag{47}$$

$$\alpha_1 = r_0(\omega^2 \epsilon_1 \mu_1 - \beta^{*2})^{\frac{1}{2}}, \quad \alpha_2 = r_0(\beta^{*2} - \omega^2 \epsilon_2 \mu_2)^{\frac{1}{2}}. \tag{48}$$

The parameter β^* is the propagation constant in the z direction and is solved from the continuity of the tangential component of field at the interface r_0, i.e. β^* is the root of

$$\frac{J_0(\alpha_1)}{\alpha_1 J_1(\alpha_1)} = \frac{\epsilon_2}{\epsilon_1} \frac{K_0(\alpha_2)}{\alpha_2 K_1(\alpha_2)}.$$

Remark 4. Here $\Theta = 0$ and $\Theta = \pi/2$ correspond to the x-polarized (HE_{11}^x) mode and the y-polarized (HE_{11}^y) mode.

In the numerical test, $\vec{\varphi}(z \equiv t = 0)$ is used as the initial condition and the exact boundary condition at $r = R$ is used. For both *Formulations A and B*, the parameters are chosen as $\Theta = 0$; the radius of core: $r_0 = 10$ μm; the radius of cladding: $R = 20$ μm; the wave length: $\lambda = 1$ μm; the wave number $k_0 = \frac{2\pi}{\lambda}$; the dielectric constant in the core: $\epsilon_1 = 1.55^2$; the dielectric constant in the cladding: $\epsilon_2 = 1.545^2$.

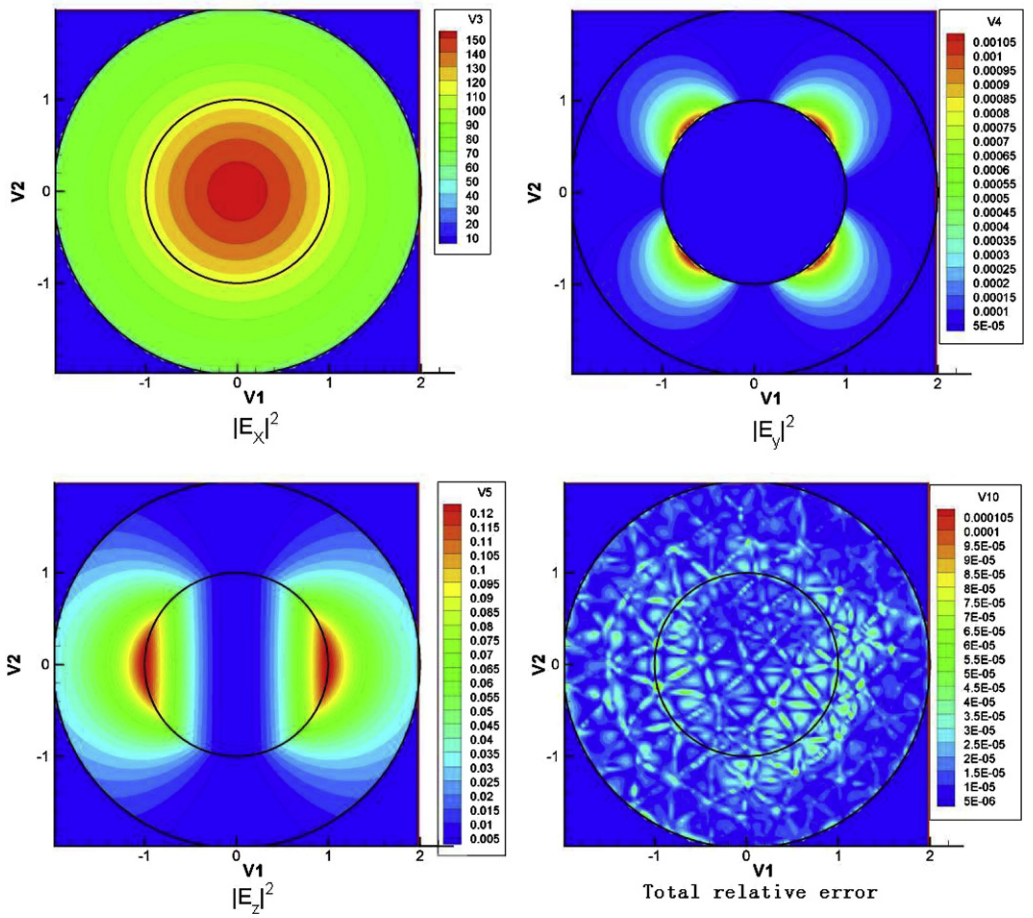

Fig. 2. Cylindrical-core case: Results by *Formulation A*.

Using *Formulation A* with a third order spatial approximation, Fig. 2 shows the intensity contours for each component and the overall relative error. *Formulation B* gives similar results. Fig. 4(a) shows the exponential convergence of the L^2 error for both *Formulations A and B*. However, compared with *Formulation A*, *Formulation B* has a larger error. That is due to the fact that divergence-free condition is used to obtain for the E_z component and the divergence condition is no longer exact after the paraxial approximation.

6.2. Propagation of LP01 modes using the magnetic field

Similarly, with the same definition for s, α_1 and α_2 as above, the LP01 mode for the magnetic component is given as

$$\varphi_1(x,y,t)=\begin{cases}\left[\frac{1-s_1}{2}J_0\left(\frac{\alpha_1}{r_0}r\right)\sin(\Theta)+\frac{1+s_1}{2}J_2\left(\frac{\alpha_1}{r_0}r\right)\sin(2\theta+\Theta)\right]G_1(t), & \text{in}\quad \Omega_1,\\ \left[\frac{1-s_2}{2}K_0\left(\frac{\alpha_2}{r_0}r\right)\sin(\Theta)-\frac{1+s_2}{2}K_2\left(\frac{\alpha_2}{r_0}r\right)\sin(2\theta+\Theta)\right]G_2(t), & \text{in}\quad \Omega_2,\end{cases}$$

$$\varphi_2(x,y,t)=\begin{cases}\left[\frac{1-s_1}{2}J_0\left(\frac{\alpha_1}{r_0}r\right)\cos(\Theta)-\frac{1+s_1}{2}J_2\left(\frac{\alpha_1}{r_0}r\right)\cos(2\theta+\Theta)\right]G_1(t), & \text{in}\quad \Omega_1,\\ \left[\frac{1-s_2}{2}K_0\left(\frac{\alpha_2}{r_0}r\right)\cos(\Theta)+\frac{1+s_2}{2}K_2\left(\frac{\alpha_2}{r_0}r\right)\cos(2\theta+\Theta)\right]G_2(t), & \text{in}\quad \Omega_2,\end{cases}$$

$$\varphi_3(x,y,t)=\begin{cases}\left(\mathrm{i}\beta^* n_1^2\frac{r_0}{\alpha_1}\right)^{-1}sJ_1\left(\frac{\alpha_1}{r_0}r\right)\sin(\theta+\Theta)G_1(t), & \text{in}\quad \Omega_1,\\ \left(\mathrm{i}\beta^* n_2^2\frac{r_0}{\alpha_2}\right)^{-1}sK_1\left(\frac{\alpha_2}{r_0}r\right)\sin(\theta+\Theta)G_2(t), & \text{in}\quad \Omega_2,\end{cases}$$

where the time dependent factors $G_1(t)$, $G_2(t)$ and two parameters s_1, s_2 are given as

$$G_1(t)=-\mathrm{i}\omega\epsilon_2 n_1^2\frac{r_0}{\alpha_1}\mathrm{e}^{\mathrm{i}(\beta_1-\beta^*)t},\quad s_1=\frac{\beta^{*^2}}{\omega^2\epsilon_1}s, \tag{49}$$

$$G_2(t)=-\mathrm{i}\omega\epsilon_2 n_2^2\frac{r_0}{\alpha_2}\frac{J_1(\alpha_1)}{K_1(\alpha_2)}\mathrm{e}^{\mathrm{i}(\beta_2-\beta^*)t},\quad s_2=\frac{\beta^{*^2}}{\omega^2\epsilon_2}s. \tag{50}$$

With the same set of parameters as used for the electric field, we test *Formulations C and D*. Fig. 3 shows the componentwise intensity contours and the overall relative error with a third order spatial approximation. Again, we omit the similar plots by *Formulation D*. Fig. 4(b) shows the exponential convergence of L^2 error for both *Formulations C and D*. Same as for the electric field, *Formulation D* produces a larger error.

Remark 5. Due to the error introduced by the paraxial approximation in the divergence condition, Formulation B (or D) will be less accurate than Formulation A (or C). However, if the extra error is within a given error tolerance, one should use Formulation B (or D) for its simplicity and saving in the computational time.

6.3. Propagation of LP01 modes in rectangular core waveguide

To show GDG–BPM's ability of handling other shapes of interfaces, we replace the cylindrical core by a square core with the same core area and still propagate the LP01 mode given in Section 6.1 for the cylindrical-core fiber. Since there is no exact solution, the numerical solutions from a coarse mesh and a fine mesh (Fig. 5(a)) are compared. The relative error plot by *Formulation A* with third order spatial approximation is given in Fig. 5(b). And the exponential decay of the L^2 error is also observed.

6.4. Propagation of LP01 modes in media with large index jump

To demonstrate the GDG–BPM's ability in dealing with large index jump, we extend our computational domain to include a layer of air next to the cladding of the cylindrical core fiber considered in Sections 6.1

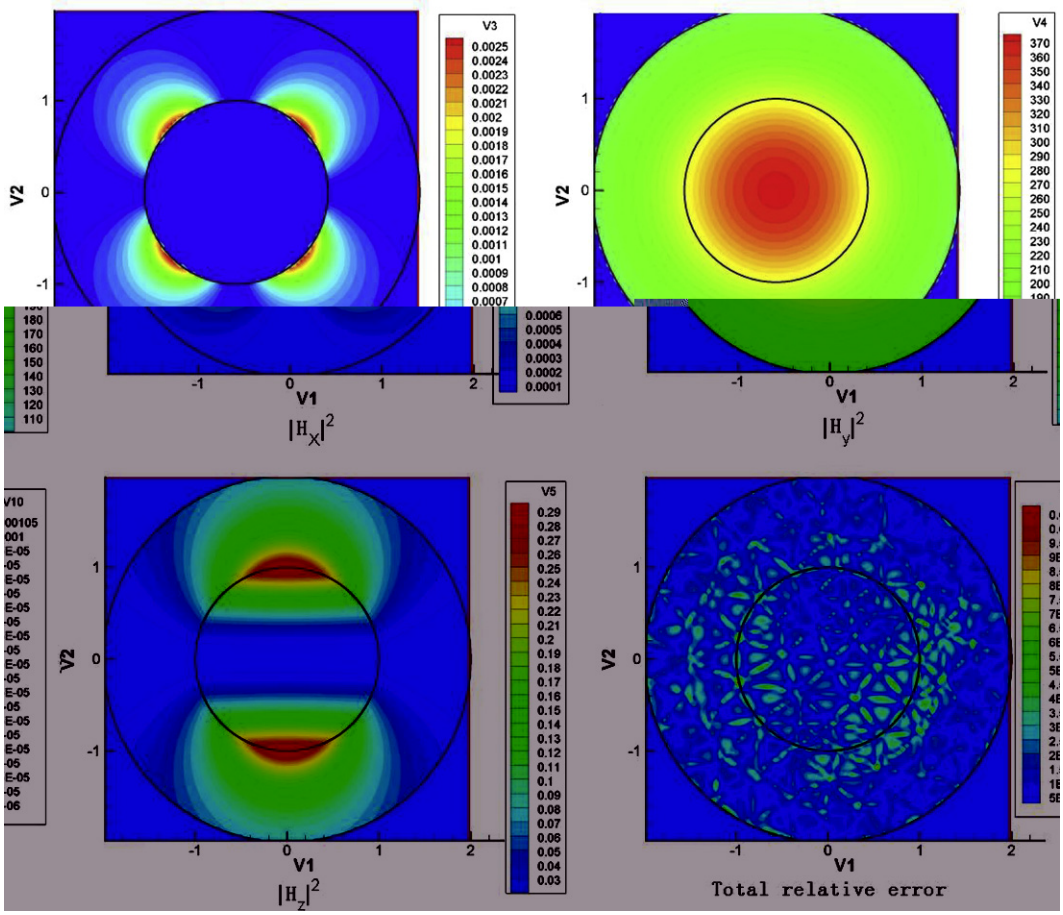

Fig. 3. Cylindrical-core case: Results by *Formulation C*.

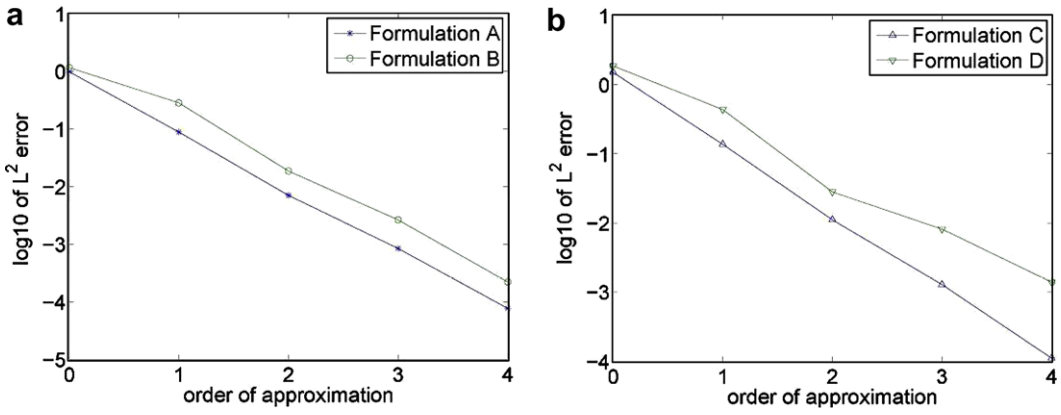

Fig. 4. Cylindrical-core case: Exponential decay of the L^2 error with increasing order of basis.

and 6.2. As shown in Fig 6(a), the central circle ($r \leqslant 10$ μm) is the core with dielectric constant $\epsilon = 1.55^2$; the next ring (10 μm $\leqslant r \leqslant$ 20 μm) is the cladding with $\epsilon = 1.545^2$ and the outer ring (20 μm $\leqslant r \leqslant$ 25 μm) is the air with $\epsilon = 1.0$. A large index jump is present at the air-cladding interface. With the transparent boundary condition used at $r = 25$ μm, the LP01 mode given in Section 6.1 is launched as the initial condition.

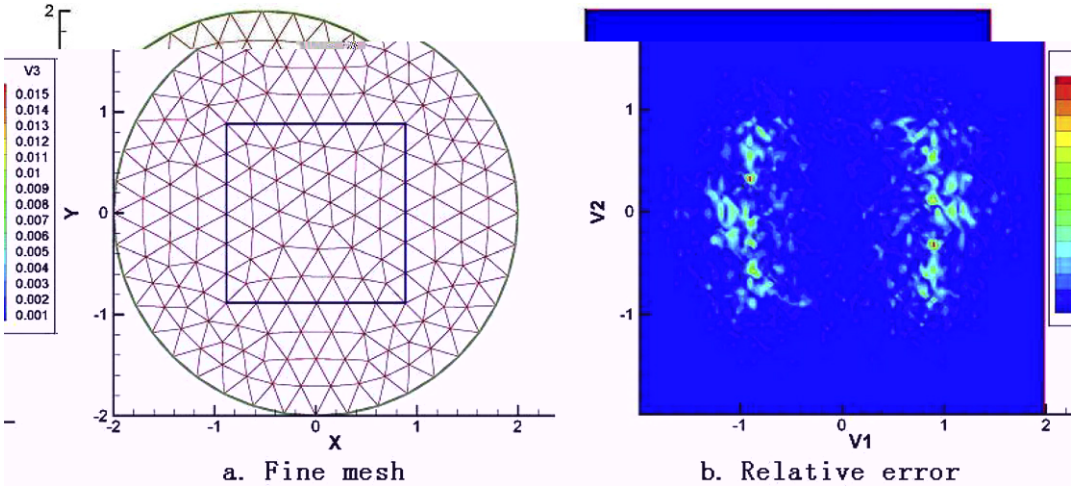

Fig. 5. Square-core case: Results by *Formulation A*.

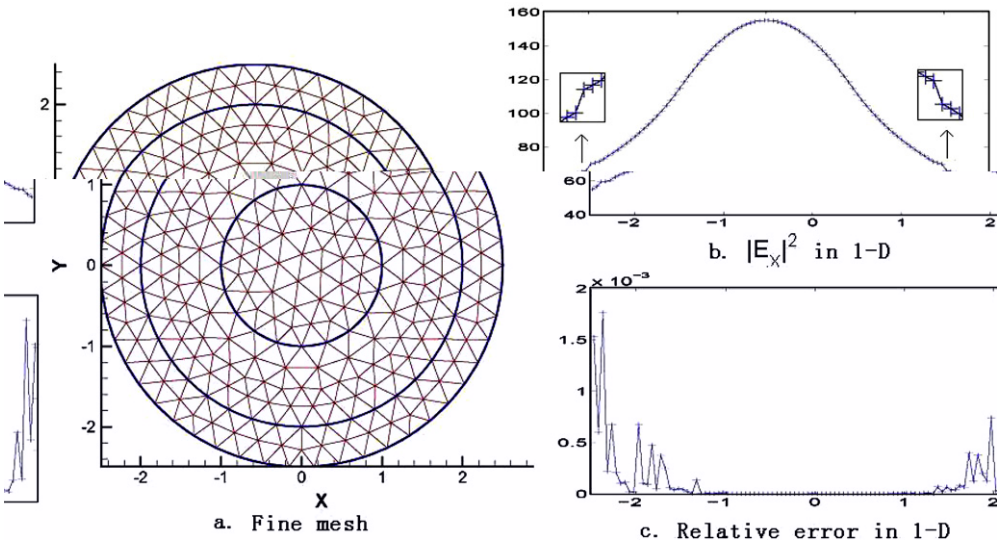

Fig. 6. Cylindrical-core with air case: Results by *Formulation A*.

Numerical convergence study by *Formulation A* with a third order spatial approximation is done on two meshes. Fig. 6(b) is the 1-D intensity plot for the E_x component, with a clear view of the discontinuity captured at the air-cladding interface. Fig 6(c) is the relative error of the intensity of the E_x component from coarse and fine meshes, which shows the high accuracy especially at the interface $r = 2$ μm of large index difference. The bigger error near the outer boundary is introduced by the transparent boundary condition.

7. Conclusion

In this paper, we proposed a new kind of beam propagation method combined with a generalized discontinuous Galerkin discretization for full vectorial simulations of electromagnetic wave propagations in inhomogeneous optical waveguides. The resulting GDG–BPM takes on four formulations for either electric or magnetic fields. Numerical results, with different shapes of interface and magnitude of jumps, demonstrate

the GDG–BPM's unique feature of handling interface jump conditions and its flexibility and high order accuracy.

Acknowledgments

The authors thank the support from the Department of Energy (grant number: DEFG0205ER25678), the NERSC Computing Award, the National Science Foundation (grant number: CCF-0513179) and DOD JTO MRI (contract W911NF-05-1-0517) for the work reported in this paper.

References

[1] M.D. Feit, J.A. Fleck Jr., Light propagation in graded-index optical fibers, Appl. Opt. 17 (24) (1978) 3990–3998.
[2] M.D. Feit, J.A. Fleck Jr., Computation of mode properties in optical fiber waveguide by a propagating beam method, Appl. Opt. 19 (7) (1980) 1154–1163.
[3] K. Fan, W. Cai, X. Ji, A generalized discontinuous Galerkin method (GDG) for Schrödinger equations with nonsmooth solutions, J. Comput. Phys. 227 (2008) 2387–2410.
[4] Y. Tsuji, M. Koshiba, N. Takimoto, Finite element beam propagation method for anisotropic optical waveguide, J. Lightwave Technol. 17 (April) (1999) 723–828.
[5] L. Thylen, D. Yevick, Beam propagation method in anisotropic media, Appl. Opt. 21 (August) (1982) 2751–2754.
[6] C.L. Xu, W.P. Huang, J. Chrostowski, S.K. Chaudhuri, A full-vectorial beam propagation method for anisotropic waveguide, J. Lightwave Technol. 12 (November) (1994) 1926–1931.
[7] A.W. Snyder, J. Love, Optical Waveguide Theory, first ed., Springer, 1983.
[8] I.M. Gelfand, N.Ya Vilenkin, Generalized Functions, Academic Press, 1977.
[9] G.A. Baker, Finite element methods for elliptic equations using nonconforming elements, Math. Comput. 31 (1977) 45–59.
[10] M.F. Wheeler, An elliptic collocation finite element method with interior penalties, SIAM J. Numer. Anal. 15 (1978) 152–161.
[11] D.N. Arnold, An interior penalty finite element method with discontinuous elements, SIAM J. Numer. Anal. 19 (1982) 742–760.
[12] D. Arnold, F. Brezzi, B. Cockburn, L.D. Marini, Unified analysis of discontinuous Galerkin methods for elliptic problems, SIAM J. Numer. Anal. 39 (5) (2002) 1749–1779.
[13] D. Funaro, D. Gottlieb, A new method of imposing boundary conditions for hyperbolic equations, Math. Comput. 51 (184) (1988) 599–613.
[14] J.S. Hesthaven, D. Gottlieb, A stable penalty method for the compressible Navier–Stokes equations. I. Open boundary conditions, SIAM J. Sci. Comput. 17 (3) (1996) 579–612.
[15] B. Cockburn, C.-W. Shu, The local discontinuous Galerkin method for time-dependent convection–diffusion systems, SIAM J. Numer. Anal. 35 (1998) 2440–2463.
[16] K. Okamoto, Fundamentals of Optical Waveguides, Academic Press, 2006.